A&A manuscript no.
(will be inserted by hand later)

Your thesaurus codes are:
09 (09.03.1 ; 09.04.1 ; 09.09.1)

ASTRONOMY
AND
ASTROPHYSICS
1.2.2008

Extinction map of Chamaeleon I molecular cloud with DENIS star counts⋆

L. Cambrésy[1], N. Epchtein[1], E.Copet[1], B. de Batz[1], S. Kimeswenger[2], T. Le Bertre[1], D. Rouan[1], and D. Tiphène[1]

[1] Observatoire de Paris, CNRS URA 264 and URA 335, F-92195 Meudon Cedex, France
[2] Institut für Astronomie der Leopold–Franzens–Universität Innsbruck, Technikerstraße 25, A–6020 Innsbruck, Austria

Received ....

Abstract. Massive, large scale star counts in the J (1.25 μm) band provided by the Deep Near Infrared Survey of the Southern Sky (DENIS) are used for the first time to draw out an extinction map of the Chamaeleon I dark cloud. We derived a $2'$ resolution map of the cloud from J star counts within an area of $1\overset{\circ}{.}5 \times 3^\circ$ around the centre of the cloud using an adaptive grid method and applying a wavelet decomposition. Possible contaminating young stellar objects within the cloud are removed, although they are shown to have a negligible effect on the counts. A comparison of our extinction map with the *cold* contribution of the IRAS 100 μm emission shows an almost perfect matching. It is shown that J star counts supersede optical counts on Schmidt plate where $A_V > 4$.

Key words: ISM : clouds – ISM : dust, extinction – ISM : individual objects : Chamaeleon

1. Introduction

The Chamaeleon I cloud is the most obscured region of the Chamaeleon dust-molecular complex. An extinction map of this cloud has been drawn out by Gregorio Hetem et al. (1988) using star counts on ESO(B) plates. It shows a maximum of $A_V \sim 6$, and the extinction profile across the cloud centre shows an abrupt growth between 2 and 6 A_V, followed by a plateau at the peak of extinction which looks like a saturation. As stars become too scarce, optical counts can no longer be used to derive the extinction accurately. Near infrared (1-2 μm) star counts are more appropriate to probe regions where $A_V \gtrsim 4$ since an extinction of 10 visual magnitudes drops to only ≈ 3 magnitudes in the J band at 1.25 μm. Massive star counts in the near infrared are made possible for the first time thanks to the large scale near infrared survey, DENIS, currently in progress (Epchtein, 1997). The aim of this paper is to investigate in detail the extinction toward the Cham I cloud using this new wealth of data.

The Cham I dark cloud is located at $b = -16^\circ$ and its current distance estimate is 140 pc (Whittet et al, 1987). Its high galactic latitude implies a small number density of background stars which limits the spatial resolution of the extinction estimation, but, on the other hand, the probability of crossing several clouds on the line of sight is low.

2. Observations

The observations presented here have been collected as part of the DENIS survey between January and May 1996 at La Silla (Chile) using the ESO 1 meter telescope equipped with the specially designed 3-channel camera (Copet, 1996). They cover an area of $1\overset{\circ}{.}45 \times 2\overset{\circ}{.}94$ centered at $\alpha = 11^{\rm h}06^{\rm m}$, $\delta = -77^\circ30^{\rm m}$ (J2000) in three bands, namely I (0.8 μm), J (1.25 μm) and $K_{\rm s}$ (2.15 μm). They consist of 13 strips each involving 180 images of $12' \times 12'$ taken at constant RA along an arc of 30° in declination. The overlap between two adjacent strips reaches 75% in the Cham I cloud because of the proximity of the south pole. Wherever a star is picked up in two adjacent strips, position and flux values are averaged. Limiting magnitudes are 18, 16 and 14 at 3σ in I, J and $K_{\rm s}$ bands, respectively, and position accuracy is $1''$ in both directions.

3. Star count method

Usually, the extinction is evaluated by comparison of star counts in the absorbed region and a nearby area assumed to be free of obscuration (Wolf diagram method). Star

Send offprint requests to: Laurent Cambresy, Cambresy@denisezg.obspm.fr

⋆ Based on observations collected at the European Southern Observatory, La Silla, Chile

counts are performed by adding up the stars up to a given magnitude (or in a given magnitude range, e.g., $\pm\frac{1}{2}$) within a grid of fixed squares. The step of the grid is a compromise between the stellar density and the spatial resolution. In other words, the spatial resolution is underestimated wherever the extinction is low, while in highly obscured areas, the content of several cells must be merged, in order to pick up enough stars.

We have developed a new method to investigate the extinction across a cloud which consists in replacing usual star counts by an estimation of the local projected star density obtained by measuring the mean distance of the x nearest stars. The most important advantage of this method is to match the local extinction: it corresponds to a star count with adaptable square size. Another very interesting advantage of the method is to provide a map with white noise. Therefore, we can simply estimate the noise by computing the standard deviation σ of the mean distance on a part of our map with no signal.

We obtain a map where each point represents the square root of the local density. The extinction is then easily derived by the relation :

$$A_\lambda = \frac{1}{a} \log \left(\frac{\overline{d_{\rm cl}}}{\overline{d_{\rm cp}}} \right)^2 \quad (1)$$

where a is defined by :

$$\log \left(\overline{d_{\rm cp}} \right)^{-2} = a \times m_\lambda + b \quad (2)$$

where m_λ is the magnitude, $\overline{d_{\rm cl}}$ the mean distance of the x nearest stars in the cloud and $\overline{d_{\rm cp}}$ the mean distance of the x nearest stars in a comparison field supposed unobscured. We found $a = 0.34$. We verified that the relation (2) is correct up to $J = 16$, i.e. our limit of completeness. Actually, we do not need a reference field to derive the extinction because the available data cover 30° of latitude and, thus, widely exceed the cloud dimension. So, we plotted the density versus the galactic latitude to interpolate the density inside the cloud for no extinction. Then we convert A_J into visual extinction using the extinction law of Cardelli et al. (1989) for $R_V = \frac{A_V}{E_{B-V}} = 3.1$. So $\frac{A_J}{A_V} = 0.282$.

A limitation to star counts behind molecular clouds, is the possible presence of young stars embedded inside the cloud itself. To draw out a reliable extinction estimate, the counts must be dominated by background stars. Therefore, we have attempted to remove these *spurious*, although interesting, objects using a colour excess criterion. A first iteration of the extinction estimation is carried out without taking into account these objects. Then, this map is used to deredden all stars, individually. Their colours $J - K$ are compared to the main sequence star at the cloud distance in a colour–magnitude diagram (K versus $J - K$). Then we flag each star which would have an extinction even greater than 5 A_V and which are likely

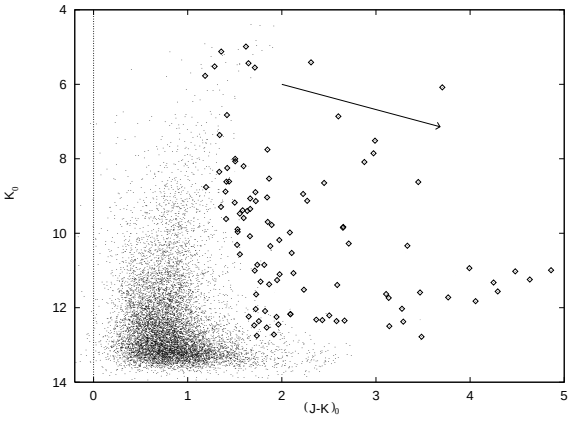

Fig. 1. Colour–magnitude diagram of dereddened stars in an area of 4.3 deg^2. Diamonds represents young stellar object candidates (100 on 30 000 stars), the arrow corresponds to the extinction vector of $A_V = 10$

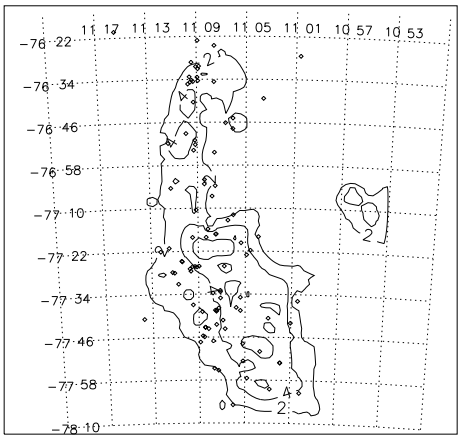

Fig. 2. Spatial distribution of young stellar object candidates. Extinction isocontours at 2, 4 and 7 A_V are overplotted

to be intrinsically very red objets. The colour–magnitude diagram is presented in Fig. 1. The spatial distribution of these flagged stars (Fig. 2) show essentially two clusters near the two $A0$ stars HD 97300 (at the north) and HD 97048 (in the centre). This result is in agreement with several studies of T–Tauri associations in the Cham I with IRAS (Assendorp et al., 1990) and ROSAT (Lawson et al., 1996). We find also several red stars farther away from the dense cores of the cloud. They could be real objects (T–Tauri, red giant), or their position in the diagram might be unreliable because of the uncertainty on the $J-K$ colour. We emphasize the fact that our criterion identifies only the classical T–Tauri, but not the so called *weak–line* T–Tauri which have no or little infrared excess. Nevertheless, this type of T–Tauri does not concentrate in the dense cores as the classical one does, so they have probably little effect on star counts. Finally, this operation removes only 0.5% of stars ($\approx$ 100 over 30 000). Counts are, thus, strongly

dominated by background stars. Then, we have built an extinction map from the cleaned counts.

We can consider our map as a digitized *image* which allows to use current technics of image processing such as the wavelet transform to restore the image and to filter the noise (Starck & Murtagh, 1994). We apply the *à trous* wavelet transform algorithm to split-off the image into 4 wavelet planes. The decomposition is made by convolving the image by a low–pass filtering matrix. The difference between the original image and the result of the first convolution gives the first plane of the wavelet transform which corresponds to the high frequency plane. Further iterations of this process provide the 4 wavelet planes and the final smooth plane.

Thus, we can use the high frequency plane to identify aberrant points and remove them in the final image in order to eliminate their contribution in all the planes, by replacing the bad pixels by the average of the surrounding 8 pixels. We are conscious that this process might result in a loss of information, but less than 0.05% pixels are actually corrected in this way.

Lastly, we filter each wavelet plane using the following method. The noise on star counts is poissonian, but taking the logarithm, as defined in equation (1) changes the statistical properties which are no longer poissonian. A Poisson noise having the standard deviation estimated in a region of the map with no signal is simulated. Then we take its logarithm and we decompose this simulated noise into wavelet planes. The estimation of the standard deviations σ_i on each plane allows an adaptable thresholding. Then we filter each plane at $3\sigma_i$.

4. Results

In order to optimize the resolution, we choose the J band and a number $x = 20$ stars to estimate the local density. The extinction is characterized at each point by the mean distance to the 20 nearest stars. In the J band the resulting spatial resolution is $1'$ for low extinction ($A_V \sim 1$) and $2'30''$ for $A_V \sim 8$. In the I band we find more than $4'$ and the K_s band is not sensitive enough. The final result is the extinction map presented in Fig. 3 with the IRAS 100 μm emission isocontours in which a *warm* contribution has been subtracted (see below). This map in false colours results from the recombination of the 4 wavelet planes.

The standard deviation of the map is $\sigma = 1.4$ magnitude. The resolution for high extinction allows to clearly identify 4 distinct maxima greater than 7 which were not resolved by the Schmidt plate analysis. The maximum is $A_V \sim 9.8$. There is no evidence of saturation. Using the relation between visual extinction and N_H column density (Savage and Mathis, 1979) we derive the mass M of the cloud for $A_V > 2$:

$$M = \alpha\mu d^2 \frac{N_{H_I}+2N_{H_2}}{A_V} \sum_i A_V^i = 280 M_\odot$$

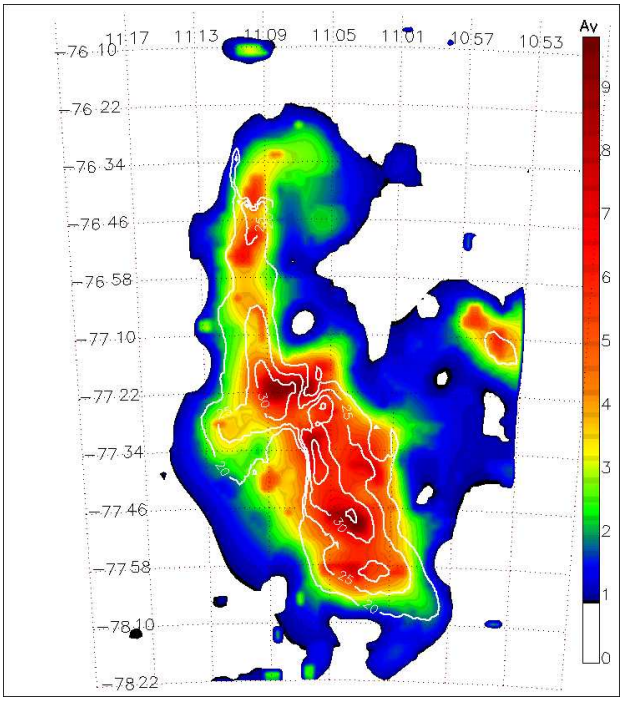

Fig. 3. Extinction map derived from J band stellar counts and cold IRAS 100 μm emission isocontours at 20, 25, 30, 35 MJy.sr^{-1} (see text)

where α is the angular size in square radian, d the distance to the cloud, and μ the mean particle mass. To calculate μ we consider a gas composed of 91.5% of hydrogen (H_2+HI) and 8.5% of helium. The mass cannot be estimated in a straightforward way for $A_V < 2$ because the slow variation of the extinction and the lower sensitivity in the J band induce important consequences on the value of the solid angle α which delineates the absorbing region, but the larger uncertainty on the mass determination comes from the distance estimate.

The extinction map that we have drawn out and the 100 μm map of IRAS have a comparable spatial resolution. It is therefore tempting to cross-correlate the 2 maps to derive some properties of the dust grains. According to Laureijs et al. (1991) the IRAS 100 μm flux consists of a *cold* and a *warm* components which can be split off into two components using the 60/100 μm colour temperature. Following Boulanger et al. (1997), the cold contribution can be written:

$$I_{\rm cold}(100\ \mu{\rm m}) = 1.67 \times (I_\nu(100\ \mu{\rm m}) - 5 \times I_\nu(60\ \mu{\rm m}))$$

Figure 3 shows that our extinction map and the cold 100 μm emission are in very good agreement. Note that the two areas with no IRAS contour ($11^{\rm h}10^{\rm m}$, $-76°34^{\rm m}$ and $11^{\rm h}08^{\rm m}$, $-77°34^{\rm m}$) are due to the presence of peculiar objects such as the *Infrared Nebula* (Schwartz & Henize, 1983) and very young stellar objects with outflows (Jones et al., 1985). This excellent correla-

tion suggests that the J extinction and the cold 100 μm emission have the same origin, a result in agreement with the Désert at al. (1990) dust model which shows that the 100 μm emission and the near infrared extinction are both caused by big grains. The warm component contribute strongly to 100 μm emission, but not much to the extinction. A plot of the cold IRAS 100 μm emission versus visual extinction is presented in Fig. 4.

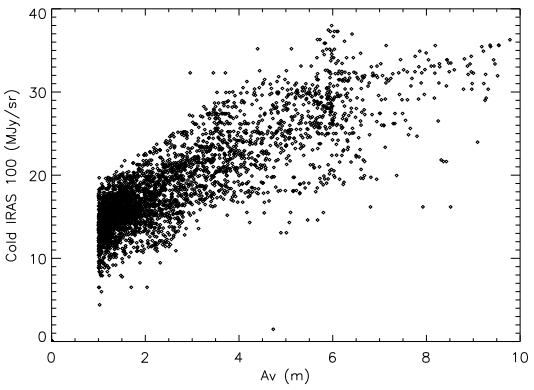

Fig. 4. Variation of cold IRAS 100 μm emission with visual extinction. Each point corresponds to a position on the map spaced of $1'$ in both directions

5. Conclusion

The extinction map of the Chamaeleon I cloud has been significantly improved for extinction greater than $4A_V$ with respect to previous maps obtained from star counts on Schmidt plates. Four distinct maxima are detected and we reach 9 visual magnitudes of extinction without degradation of the resolution. This result has been obtained both by exploiting the massive star counts in the J band provided by DENIS, and by applying a variant of the classical star count method which is adapted to large variations of extinction and a wavelet analysis of the extinction map. Moreover, DENIS give us the opportunity to investigate the cloud at a larger scale than the earlier investigations which were limited to small regions around the visible reflection nebulae.

The comparison with the cold IRAS 100 μm is striking. Each of the 3 most important extinction maxima corresponds to a peak of cold IRAS emission. The IRAS flux is therefore a good indicator of extinction. We plan further investigations of the relation between the cold IRAS emission and extinction when new CO observations at a comparable spatial resolution will be available.

Finally we stress the fact that our map has been derived from J star counts converted to visual extinction with $R_V = 3.1$. This value of 3.1 is the standard estimate for diffuse interstellar medium, but it can reach 5.5 in dense molecular cloud cores (Whittet et al., 1987). According to Cardelli et al. (1989) :

$$\frac{A_J}{A_V} = 0.4008 - \frac{0.3679}{R_V}$$

So, we obtain 0.282 for $R_V = 3.1$ and 0.334 for $R_V = 5.5$. This means that we overestimate the extinction by a factor 1.18 if we choose $R_V = 3.1$ rather than 5.5. Extinction is generally expressed in visual magnitudes. This choice is not the best because the extinction law in the visible range depends on the composition of the medium. On the other hand, the extinction law in the infrared seems universal. Therefore, it should be better to refer the extinction to near infared magnitudes. Lastly, it appears that J DENIS data with a detection limit of $16^{\rm th}$ magnitude are better adapted to investigate the obscuration of regions where the extinction is larger than 4 magnitudes, rather than the Schmidt plate even at a usual detection limit of $22^{\rm nd}$ magnitudes.

Acknowledgements. The DENIS team is warmly thanked for making this work possible and in particular the operations team at La Silla headed by P. Fouqué. The DENIS project is supported by the *SCIENCE and the Human Capital and Mobility* plans of the European Commission under grants CT920791 and CT940627, the European Southern Observatory, in France by the *Institut National des Sciences de l'Univers*, the Education Ministery and the *Centre National de la Recherche Scientifique*, in Germany by the State of Baden–Wurttemberg, in Spain by the DGICYT, in Italy by the Consiglio Nazionale delle Ricerche, in Austria by the Science Fund (P8700-PHY, P10036-PHY) and Federal Ministry of Science, Transport and the Arts, in Brazil by the Fundation for the development of Scientific Research of the State of São Paulo (FAPESP).

References

Assendorp R., Wesselius P.R., Whittet D.C.B., Prusti T., 1990, MNRAS 247, 624.
Boulanger F., Bronfman L., Dame T.M., Thaddeus P., 1997 submitted
Cardelli J.A., Clayton C., Mathis J.S., 1989, ApJ 345, 245.
Copet E., 1996, Thesis of University of Paris 6.
Désert F.-X., Boulanger F., Puget J.L., 1990, A&A 237, 215.
Epchtein N. et al., 1997, The ESO Messenger n^o 87, in press
Epchtein N., 1997, *Proc. of the* 2^{nd} *Euroconference on the impact of large scale near infrared surveys, eds. F. Garzon, N. Epchtein, A. Omont, W.B. Burton, P. Persi*, Ap&SS Library, Vol 210, p15, Kluwer Ac Pub.
Gregorio Hetem J.C, Sanzovo G.C., Lépine J.R., 1988, A&AS 76, 347.
Jones T.J. et al. 1985, AJ 90, 1191.
Laureijs R.J., Clarck F.O., Prusti T., 1991, ApJ 185, 372.
Savage B.D., Mathis J.S., 1979, ARA&A 17, 73.
Schwartz R.D., Henize K.G., 1983, AJ 88, 1665.
Starck J.L., Murtagh F., 1994, A&A 288, 342, 348.
Lawson W.A., Feigelson E.D., Huenemoerder D.P., 1996, MNRAS 280, 1071.
Whittet D.C.B., Kirrane T.M., Kilkenny D., Oates A.P., Watsonf G., 1987, MNRAS 224, 497.

This article was processed by the author using Springer-Verlag
LaTeX A&A style file *L-AA* version 3.